

Design and implementation of the planar inverted-F antenna using computer simulation technology for wireless applications

Randa Nael Adel*, Ali Hasan Khidir

Department of Physics, College of Science, University of Baghdad, Baghdad, Iraq

(Communicated by Ehsan Kozehgar)

Abstract

The Planar Inverted-F antenna (PIFA) is becoming more popular in the new multi-band mobile phone industry for transceiver systems of wireless communication systems. The purpose of this paper is to design and implement a planar inverted-F antenna for wireless communication. This device can work in the S-band resonance frequency range. Because the antenna is a quarter wavelength, the antenna size and return loss are reduced. The practical results of the used antenna showed that the return loss is about 34.20 dB, the voltage Standing Wave Ratio (VSWR) is 1.18258, and the bandwidth is 220 MHz. Theoretically, the directivity, gain, and input impedance values were also calculated as 5.617 dB, 5.247 dB, and 50 Ω , respectively. Therefore, the desired antenna is considered to perform well in terms of return loss and voltage. It can be utilized in Bluetooth, Wi-Fi, and Long Term Evolution (LTE) applications in fourth-generation cellular communications (4G).

Keywords: Flame Retardant-4 (FR-4), 4G, PIFA, Computer Simulation Technology (CST), Long Term Evolution (LTE).

2020 MSC: 76F65, 68M18

1 Introduction

The evolution of wireless communication systems in recent years is a result of their small size and wide technologies. Wireless devices offer multiple frequency bands and provide large bandwidth. As a result, we need a small antenna that supports multiple frequency bands and has wide-range coverage. The Inverted Planar F antenna (PIFA) has a small body that provides good performance [7, 4]. Planar Inverted-F antenna (PIFA) is becoming more and more popular in the mobile market, as illustrated in fig. 1 [5] due to its low profile, omnidirectional style, and low cost [8, 2]. Because wireless devices have limited space, we kept the size of this type of antenna modest and ideal for portable wireless units without losing performance. In terms of bandwidth and radiation patterns, the radiation pattern should be near to omnidirectional and cover the required operating frequency ranges for the IEEE 802.11b/g/n standard [12]. Wireless technologies IEEE 802.11b and IEEE 802.11g have gained popularity in wireless Ethernet networks due to the cost reductions and enhanced performance given by Bluetooth and wireless digital phones [10, 9]. In telecommunications, this type of antenna has been used in technology (LTE) which is a standard for wireless broadband communications for mobile devices and data stations [13].

*Corresponding author

Email addresses: randanael17@gmail.com (Randa Nael Adel), alzurfi.ahali@gmail.com (Ali Hasan Khidir)

In this paper, we will look at the antenna design and construction for (4G) cellular mobile devices as well as the applications of wireless communication systems. There was a high quality in using this antenna to work within the desired frequency range that the phone would be able to accommodate. Therefore, the results showed the quality of the antenna designed and implemented to work within the S-band frequency. MATLAB, (CST), and computer numerical control (CNC) were used to design and implement this target for the desired antenna.

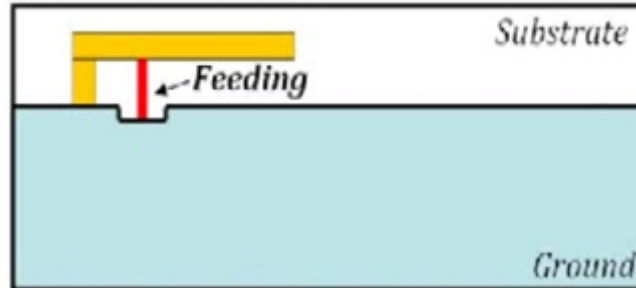


Figure 1: Inverted F-shaped antenna [3]

2 ANTENNA THEORETICAL

In this work, by equation 1, the proposed PIFA with a resonant frequency (F) of 2.35 GHz was calculated by MATLAB R2015a software (version 8.5). Modifiers 2 and 3 refer to the radiated patch length of the antenna used and the wavelength, respectively. Between the ground and patching layers is FR-4 insulating material that is 0.035 mm thick. Then the component is simulated by adjusting the input impedance 50Ω to match the antenna tuning [15].

$$F = \frac{c}{4(W + L)} \quad (2.1)$$

Where F represents the desired resonant frequency, L and W denote length and width of the radiated patch respectively, and c denotes speed of light.

$$L = \frac{c}{4F\sqrt{\epsilon_r} + W} \quad (2.2)$$

$$\gamma = \frac{c}{F} \quad (2.3)$$

Where ϵ_r is dielectric constant and γ is the wave length. The prior equations 2.2 and 2.3 were coded in the form of a GUIDE, as seen in Fig (1). Figure 2 represents the inputs and outputs of the most important parameters that were used to design the desired antenna. Where the values of the resonant frequency were 2.35 GHz, the dielectric constant (4.3), and the width (9) from which the required antenna was designed and implemented.

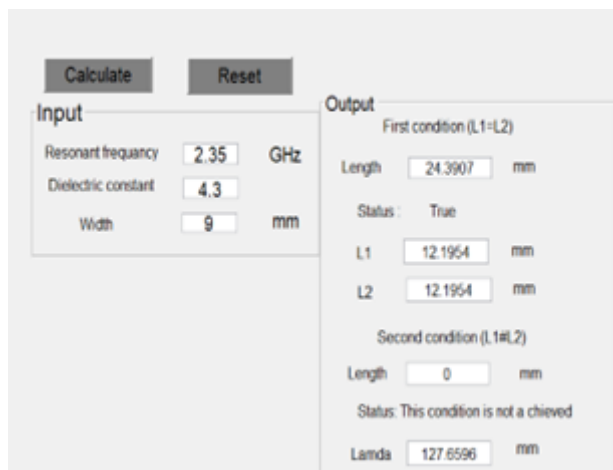


Figure 2: Calculate the input and output of the desired antenna using MATLAB [1]

Table 1: Shows all parameters of the proposed antenna

Parameter	Symbol	Value	Dimensions
Resonant frequency	F	2.3	GHz
Dielectric constant	ϵr	4.3	-
Width	W	9	mm
Length	L	24.3907	mm
Wavelength	λ	127.6596	mm
Length of radiating element	L1	12.1954	mm
Width of radiating element	L2	12.1954	mm

3 RESULTS AND DISCUSSION

3.1 Simulation Results

The simulation of Figure 3 was built using Computer Simulated Microwave Technology (CST) (version 2019). The figure shows the actual dimensions of the desired antenna. The antenna is made of a 1,356 mm thick FR-4 with a dielectric constant (ϵr) of 4.3.

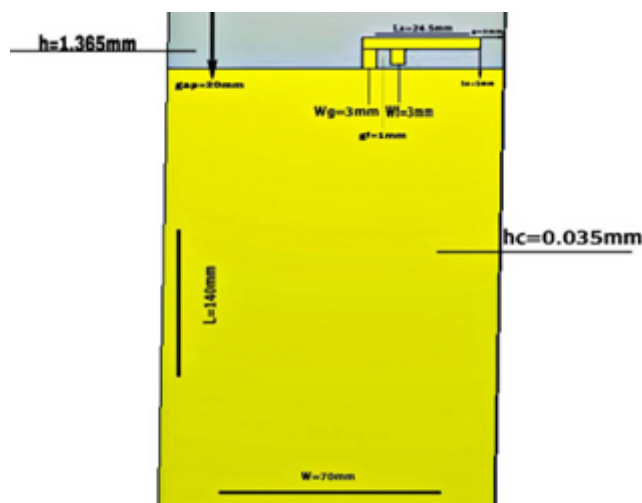


Figure 3: Structure of the proposed PIFA with all measured dimension values

Table 1 displays the parameters needed to develop and test the intended antenna with the Microwave Studio software's computer simulation technology (CST).

Table 2: Detailed dimensions of suggested PIFA

Parameter	Symbol	Dimensions
Length of ground	L	140
Substrate Thickness	h	1.365
Width of ground	W	70
Width of cut	gap	20
Length of antenna	La	24.5
Height of the antenna above the ground	ha	5
Width of feed	wf	3
Gap feed	gf	1
Width antenna	wa	3
Gap antenna	ga	3
Copper thickness	hc	0.035
Antenna distance from the edge of the substrate	g	5
Line width with ground	wg	3

3.1.1 Return loss

Figure 4 depicts a line graph between the simulated return loss values and frequency for each frequency found within the range (from 1 GHz to 5 GHz) using CST microwave program. Because of the logarithmic equation that converts fractional integers into negative real values, all RL values are negative. The RL values are near to zero in the limited region between (1 GHz and 1.49 GHz), indicating that the majority of the incident power has been reflected to the source. As a result, the antenna in this area is inoperable. After 1.54 GHz, the curve begins to drop logarithmically, eventually reaching 2.35 GHz. This shows that the antenna is progressively responding to these frequencies. Following that, the RL values steadily increase until the possibility of the antenna of response disappears.

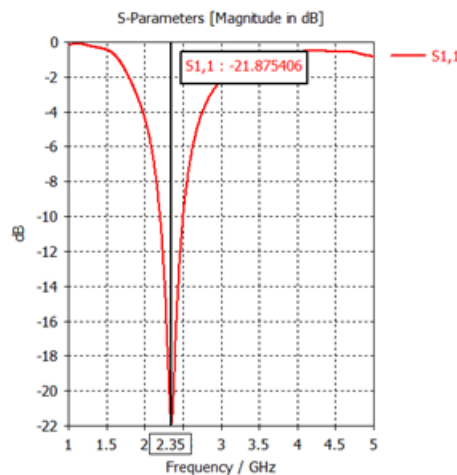


Figure 4: Return loss of the PIFA

3.1.2 Bandwidth

Figure 5 depicts the manual computation of the working zone bandwidth through the return loss. Several additional lines have been added to establish the exact region. The antenna work area is determined by placing a horizontal solid line at 10 dB. The second horizontal solid line at 20.8 dB is ignored in this study since it is outside the scope of our investigation. The frequency work space is also determined by the two vertical solid lines. The difference in

frequency between a high frequency (2.5043 GHz) and a low frequency (2.2024 GHz) yields a bandwidth of 0.3019 GHz or 301 MHz.

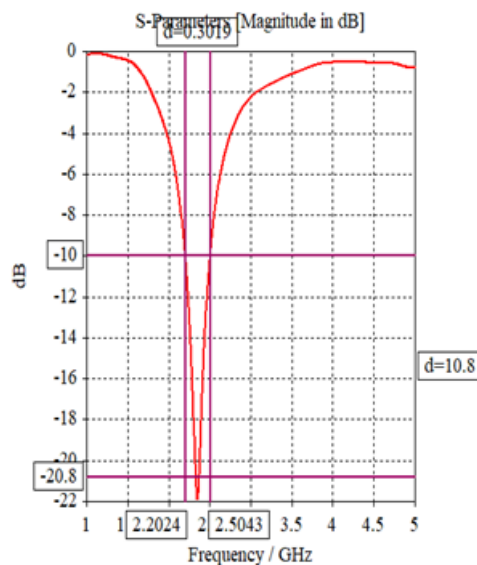


Figure 5: Band width of the PIFA

3.1.3 VSWR

Figure 6 shows the results of the VSWR parameter at the same frequency range as RL. CST microwave studio software calculated the VSWR values automatically. The minimal VSWR value is 1.1752855, which corresponds to a frequency of 2.35 GHz. The reflected voltage steadily decreases as the VSWR values fall from 153 to 1.1752855 in the left side of the line graph. The reflected voltage values are raised on the right side of the graph from 1.1752855 to VSWR value 10. High VSWR values on both sides suggest that standing waves have been set in unwanted frequencies. Because the minimal value of VSWR is close to one, the matching between source and antenna impedances is almost optimal. For a decent radiator, the voltage standing wave ratio (VSWR) should be 2:1. Figure 6 shows a gain of 5.247 dB with a VSWR value of 1.1752855 suggesting strong impedance matching (perfect matching VSWR = 1), implying that practically all input power may be transferred.

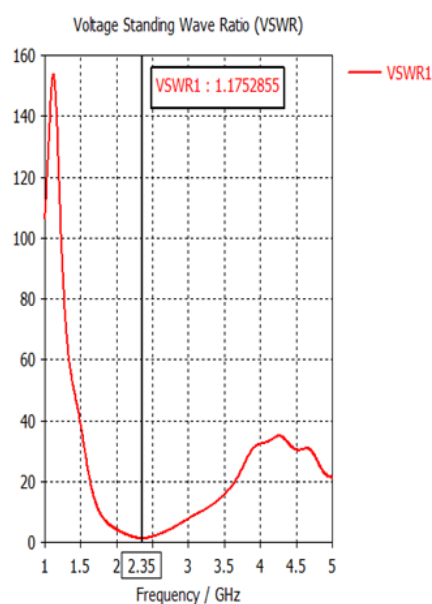


Figure 6: VSWR OF THE PIFA

3.1.4 Input Impedance

The theoretical results of the input impedance antenna used with CST microwave studio software is represented in Figure 7. The value of Z_{in} is 50Ω at the 2.35 GHz for operating frequency. This value is so close to the reference impedance value (50Ω).

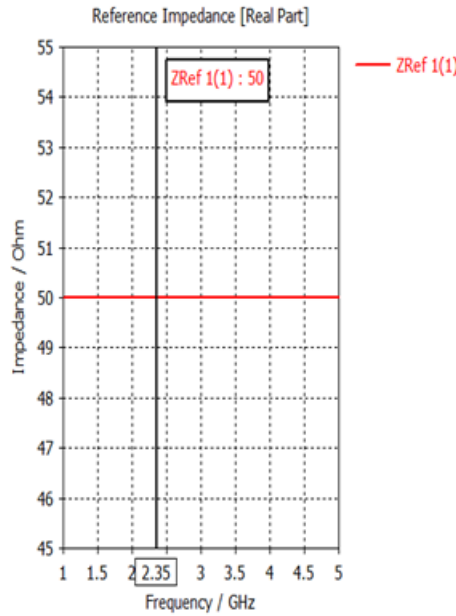


Figure 7: The PIFA input impedance

Figure 8 depicts the antenna’s far-field emission patterns. This shows that the gain is around 5.247 dBi. As a result, the gain polar plots using Smith chart show that the gain is 5.25 dBi when $\theta = 90^\circ$, as shown in Fig 9.

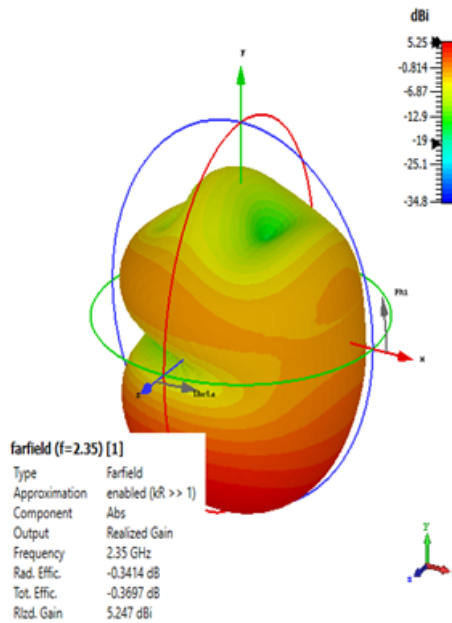
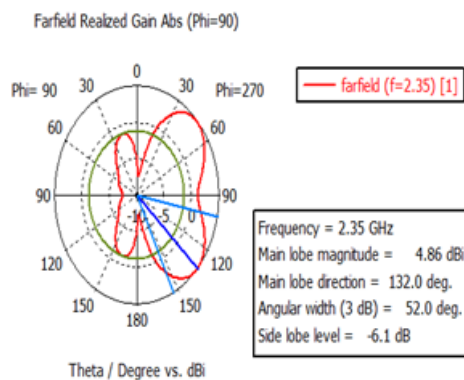


Figure 8: Gain of the PIFA

Figure 9: Polar plots of gain at $\Phi = 90^\circ$

Figures 10 and 11 shows the 3D radiation pattern and the polar plots of the trend using Smith's chart where it is noticed that the radiative directivity is 5.25 dB when the value of Φ is equal to 90° . These values are considered the best in relation to the results of others [6].

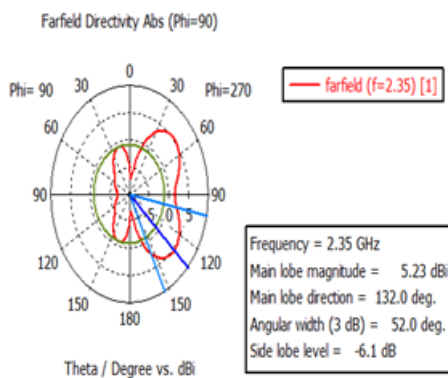
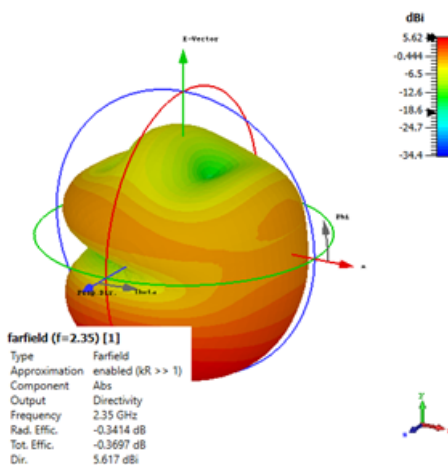
Figure 10: Polar plots of directivity at $\Phi = 90^\circ$ 

Figure 11: 3-D radiation pattern of directivity

3.2 Experimental Results

The PIFA was built on a flame retardant-4 substrate with a dielectric constant (ϵ_r) of 4.43 and a thickness (h) of 1.356 mm. The CNC machine (Acetek AKM6090) approach is utilized to fabricate the printed circuit board (PCB)

of the desired antenna, as shown in Fig. 12. The antenna test results were quite close to the modeling findings used in this research, and they are regarded good when compared to previous results [3].



Figure 12: Front view of the PIFA

The antenna was tested experimentally with a Network analyzer (E5071C) as shown in Fig. 13. According to Fig. 13, the experimental result's return loss has grown to -34.20 dBi. It is also noted that the resonant frequency in the practical result was slightly lower and equal to 2.22 GHz. This value is good compared to the results of others [14].

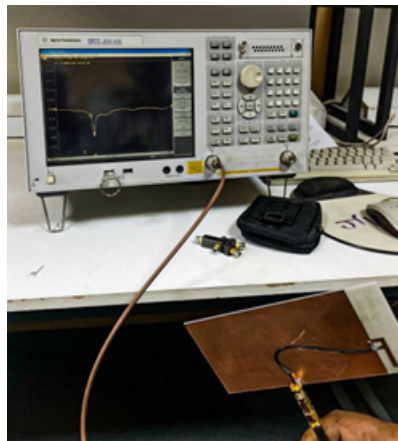


Figure 13: Test the desired antenna with a network analyzer

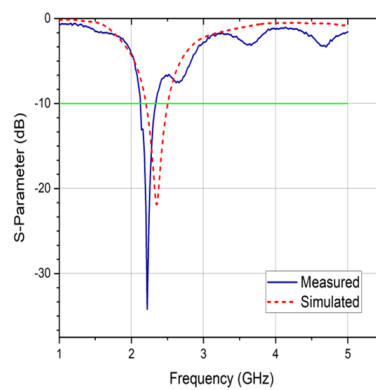


Figure 14: Return loss values for the simulation and the manufactured results

Figure 15 shows the simulation results and the practical value of the manufactured antenna. From the figure it is shown that the practical value of VSWR is 1.18258, which is considered very close to the simulation value, thus verifying the quality of the work of the designed and ported antenna. Because the practical value of antenna quality is less than 2. Therefore the antenna works well within the frequency band of the resonant frequency at 2.35 GHz. This value is good compared to the results of others [11].

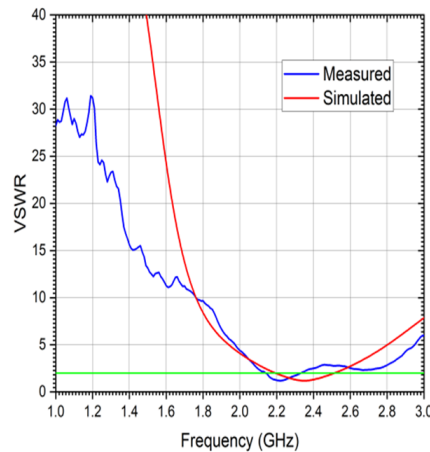


Figure 15: The simulated and fabricated results of the VSWR

Table 3 provides the theoretical and practical values of the needed antenna's resonance frequency, return loss, bandwidth, and VSWR. The slight difference in the theoretical and practical values of the required antenna is caused by the fact that the ends of the antenna edges are blunt and contain scratches for these edges due to CNC machining.

Table 3: The PIFA simulation and experimental results

Results	Simulated	Experimental
Frequency of Resonance (GHz)	2.35	2.22
Return loss (dB)	-21.88	-34.20
Bandwidth (MHz)	301	220
VSWR	1.17528	1.18258

4 Conclusion

It can be concluded from this work that the manufactured antenna works within the frequency band of the fourth generation within the frequency bands of this generation, it can be seen through the amount of the resonant frequency that was practically obtained is 2.22 GHz. Also, the practical results of return loss, bandwidth, and VSWR of this antenna were good values for antenna work which makes the antenna work very efficiently. As shown in Table 3 above.

References

- [1] A.B. Balametov, E.D. Halilov, AK Salimova, and FG Iskenderov, *Algorithm and matlab-based program for modeling the nodal electricity prices*, Int. J.Tech. Phys. Prob. Engin. **12** (2022), no. 1, 20–24.
- [2] Y.F. Cao, S.W. Cheung, and T.I. Yuk, *A multiband slot antenna for gps/wimax/wlan systems*, IEEE Trans. Antenna Propag. **63** (2015), no. 3, 952–958.
- [3] H.T. Chattha, Y. Huang, and Y. Lu, *Pifa bandwidth enhancement by changing the widths of feed and shorting plates*, IEEE Antennas Wireless Propag. Lett. **8** (2009), 637–640.
- [4] A.P. Dabhi and S.K. Patel, *Response of planar inverted f antenna over different dielectric substrates*, Int. J. Sci. Technol. Res. **3** (2014), no. 4, 114–117.

-
- [5] Walid El Hajj, Christian Person, and Joe Wiart, *A novel investigation of a broadband integrated inverted-f antenna design; application for wearable antenna*, IEEE Trans. Antennas Propag. **62** (2014), no. 7, 3843–3846.
- [6] M. El Halaoui, H. Asselman, A. Kaabal, and S. Ahyoud, *Design and simulation of a planar inverted-f antenna (pifa) for wi-fi and lte applications*, Int.J. Innov. Appl. Stud. **9** (2014), no. 3, 1048–1055.
- [7] A. Kocak, M. C. Taplamacioglu, and H. Gozde, *General overview of area networks and communication technologies in smart grid applications*, Int. J. Tech. Phys.l Prob. Engin. **13** (2021), no. 1, 103–110.
- [8] C.M. Krishna and P.J. Vijay, *Design and analysis of integrated pifa for wireless applications*, Int. J. Re. Electron. Comput. Engin. **6** (2018), no. 3, 2348–2281.
- [9] N. Kumar and G. Saini, *A novel low profile planar inverted-f antenna (pifa) for mobile handsets*, Int. J. Sci. Res. Pub. **3** (2013), no. 3.
- [10] C.-W. Ling, C.-Y. Lee, C.-L. Tang, and S.-J. Chung, *Analysis and application of an on-package planar inverted-f antenna*, IEEE Trans. Antennas Propag. **55** (2007), no. 6, 1774–1780.
- [11] S.D. Mallanna, K. Viswanath, and P.K.B. Rangaiah, *Design and analysis of high gain planar inverted-f antenna (pifa) for wimax and nomadic applications*, Sixth Int. Conf. Wireless Commun.Signal Process. Network. (WiSPNET), IEEE, 2021, pp. 6–10.
- [12] K. Pahlavan and P. Krishnamurthy, *Evolution and impact of wi-fi technology and applications: A historical perspective*, Int. J. Wireless Inf. Networks **28** (2021), 3–19.
- [13] M. Singh, V. Marwaha, A. Thakur, H.S. Saini, and N. Kumar, *Design of a low return loss planar inverted f antenna (pifa) for 4g & wlan applications loaded with metamaterial lens*, 3rd Int. Conf. Signal Process. Integrated Networks (SPIN), IEEE, 2016, pp. 539–543.
- [14] R.K. Verma, *Bandwidth enhancement of an inverted f-shape notch loaded rectangular microstrip patch antenna for wireless applications in l and s-band*, Wireless Pers Commun. **125** (2022), 861–877.
- [15] K.L. Wong, *Planar antennas for wireless communications*, Microw. Opt. Eng., ser. Wiley Series in Microwave and Optical Engineering, 2003, pp. 26–69.